COMBINING TWO PHASE CODES TO EXTEND THE RADAR UNAMBIGUOUS RANGE AND GET A TRADE-OFF IN TERMS OF PERFORMANCE FOR ANY CLUTTER

Timothée Rouffet [1],[3] *Eric Grivel* [3] *Pascal Vallet* [3] *Cyrille Enderli* [2] *Stéphane Kemkemian* [2]

THALES Systèmes Aéroportés S.A., [1]Pessac, FRANCE, [2]Elancourt, FRANCE
[3]Université de Bordeaux, Bordeaux INP, IMS, UMR CNRS 5218, Talence, FRANCE

ABSTRACT

This paper deals with a phase-coded waveform which combines two binary phase codes, each impacting on specific properties of the radar receiving channel. After giving a detailed analysis of the expression of the received signal after processing when the Gaussian clutter is modeled by a pth-order autoregressive process, we focus our attention on the choice of the two phase codes: one aims at increasing the unambiguous range whereas the other is chosen by taking into account several criteria such as the detection performance. For this purpose, we suggest determining the Pareto fronts of 1st, 2nd and 3rd orders by means of an exhaustive search. Given the three Pareto fronts for different types of clutters simulated by making the AR parameters vary, we provide an automatic way to determine, before embedding it, the most robust phase codes using a fuzzy logic operator.

***Index Terms*—** phase codes, autoregressive modelling, Pareto fronts, fuzzy logic, radar, unambiguous range.

1. INTRODUCTION

The primary mission of a radar, as stated in its acronym *RAdio Detection and Ranging*, is to detect a target. However, the design of the waveform and its processing must be addressed by taking into account several issues such as the detection performance despite of the clutter, the range and speed ambiguity resolution[1], etc.

Let us first look at the approaches that have been proposed to maximize the probability of detection. When the received signal is altered by thermal noise only, the matched filter aims at maximizing the signal-to-noise ratio. In that case, all the waveforms with a given energy provide the same probability of detection [1]. When the received signal is disturbed by a colored Gaussian clutter and a thermal noise, De Maio *et al.* [2], [3] considered a pulse train with an interpulse phase code and addressed its optimization by combining the detection performance and a similarity constraint with a given phase code such as Barker codes, P3 codes, etc. These codes have been chosen as references because they lead, after matched filtering, to the desired properties in terms of sidelobe height [4]. However, in the presence of clutter, the matched filter alone is no longer the "optimal" processing. Indeed, maximizing the signal-to-clutter-plus-thermal-noise ratio has to be done in two filtering steps: the first one whitens the colored clutter whereas the second one is a filter matched to the delayed and Doppler-shifted signal after the whitening filter. In that case, the probability of detection is a function of the transmitted signal and the covariance matrix of the interference [1]. Therefore, Patton *et al.* [5] suggested maximizing the signal-to-interference-plus-noise ratio and added a constraint on the sidelobes of the optimal waveform autocorrelation function. In [6], assuming the disturbance covariance matrix is known, the authors addressed the waveform design through a multiobjective approach in order to combine range and Doppler resolution capabilities. More recently in [7], we investigated the following scenario: the received signal is first processed in a low-resolution "receiving channel". When a detection occurs, the received-signal samples are reprocessed in a high-resolution receiving channel to obtain a range profile. This scenario has the advantage of reducing the computational cost of the whole processing chain. In addition, the target illumination time is increased. Assuming a colored Gaussian clutter with thermal noise, we addressed the waveform design by optimizing several criteria, such as the probability of detection. Given this multiobjective optimization issue, we proposed to search the Pareto front by modelling the clutter with a first-order autoregressive (AR) process.

In the above approaches, the range ambiguity issue is not taken into account. In current radar, this issue has been addressed by changing the PRF according to the configuration, i.e. air-to-air, air-to-ground, and to the needs, i.e. long range detection, mid-range tracking, etc. Another way to address the ambiguities is to consider two trains of pulses with two different PRFs. The resulting PRF is the least common multiple of the two PRFs [8]. When there is no clutter and only thermal noise, a third possibility consists in using an interpulse phase code the autocorrelation of which has specific properties in terms of sidelobes. For instance in [9], Levanon uses a pair of mismatched codes such that their circular cross-correlation has no sidelobes up to a certain range. However, the circularity implies that the first and the last sequences cannot be used for detection.

In this paper, we suggest combining inter and intrapulse phase codes processed in a single receiving channel. This combination has the following advantages: the interpulse code is used to extend the radar unambiguous range whereas the intrapulse code is used to drive the performance of the receiving channel. Given this scenario, our contribution is threefold:

1/ We provide a detailed analysis of the expression of the received signal after processing when the clutter is modeled by a pth-order AR process (AR(p)). Such a model has the advantage of modelling the clutter with few parameters. By modifying the AR parameters, different correlation properties for the clutter can be simulated. In addition, the inverse of its covariance matrix has an analytical form based on the AR parameters;

2/ Using the analytical expression of the received signal after processing, we present a way to select both codes;

3/ We propose an automatic way to *a priori* choose the intrapulse phase code. For each type of clutter, we define the Pareto fronts of

[1]In pulse-Doppler radar, the target range is determined modulo a parameter called "range ambiguity" inversely proportional to the pulse repetition frequency (PRF). The target speed is determined modulo a parameter called "speed ambiguity" proportional to the PRF. Therefore, the user has to choose between range and speed ambiguities.

1st, 2nd and 3rd orders and compute them. Then, we deduce the percentages of presence of each code in the three sets of Pareto fronts. Finally, we combine them with a fuzzy logic operator. The most relevant codes correspond to those which remain the most often on the Pareto fronts when the correlation properties of the clutter vary. Since the computation of the Pareto fronts can be carried offline, i.e. not on the embedded system, the computational cost required for the selection of the intrapulse phase code is not a constraint.

The remainder of this paper is organized as follows: in section 2, we present the phase-coded waveform and its processing. Then, we analyze the influence of an AR(p) clutter model on the received signal. Section 3 deals with the selection of the two codes and simulations results are provided in section 4.

2. HYBRID WAVEFORM MODEL AND PROCESSING AT THE RECEIVER

2.1. Transmitted waveform and its processing at the receiver

Let us study the waveform $s(t)$ which is a train of K phase-coded pulses combining an intra and an interpulse binary phase codes given by:

$$s(t) = \sum_{k=0}^{K-1} c_k p(t - kT_r) \tag{1}$$

where $c_k = \pm 1$ is the k^{th} element of the interpulse phase code $\mathbf{c}$ of length K, T_r the pulse repetition interval (PRI) and $p(t)$ the pulse of duration T defined by:

$$p(t) = \sum_{m=0}^{M-1} d_m u(t - mT_c) \tag{2}$$

with $d_m = \pm 1$ the m^{th} element of the intrapulse phase code $\mathbf{d}$ of size M and $u(t)$ the rectangular function of duration T_c. For the sake of clarity, an illustration is presented in Fig. (1) where $N = \frac{T_r - T}{T}$.

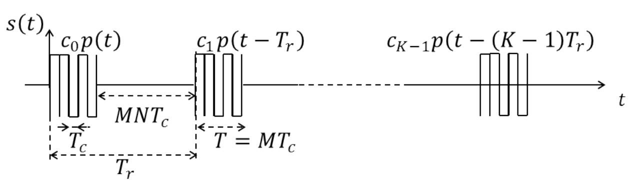

Fig. 1. Proposed waveform with inter and intrapulse phase codes

Then, we consider a point target whose range is proportional to the travel time τ_0 of the emitted signal. τ_0 can be expressed as:

$$\tau_0 = \ell_0 T_c + \epsilon_0 \text{ with } 0 \leqslant \epsilon_0 < T_c \ , \ 0 \leqslant \ell_0 < KNM \tag{3}$$

Assuming a known Doppler frequency and under the narrowband hypothesis, the proposed processing on the received signal $y(t)$ is given in Fig. (2) and aims at estimating ℓ_0. In the following, ℓ denotes a candidate range gate and is such that $0 \leqslant \ell < KMN$.

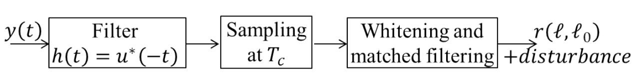

Fig. 2. Processing at the receiver

Given Fig. (2), the received signal after processing is the sum of a function r and a term of disturbance which contains the thermal noise and the clutter after processing. It can be shown [7] that r satisfies:

$$r(\ell_0, \ell) = (\mathbf{c} \otimes \mathbf{e}_1 \otimes \mathbf{d})^H (\mathbf{J}^{\ell_0})^H \mathbf{M}^{-1} \mathbf{J}^{\ell} (\mathbf{c} \otimes \mathbf{e}_1 \otimes \mathbf{d}) \tag{4}$$

where $.^H$ denotes the conjugate transpose, $\otimes$ the Kronecker product, $\mathbf{e}_1$ the $N \times 1$ vector defined as $\mathbf{e}_1 = [1\ 0\ ...\ 0]^T$, $\mathbf{J}$ the $KMN \times KMN$ "shift" matrix which has ones on the first subdiagonal and zeros elsewhere, and $\mathbf{M}$ the covariance matrix defined by:

$$\mathbf{M} = \mathbf{\Gamma} + \sigma^2 \mathbf{I} \tag{5}$$

with $\mathbf{\Gamma}$ the covariance matrix of the clutter, $\mathbf{I}$ the $KMN \times KMN$ identity matrix and σ^2 the variance of the additive thermal noise.

2.2. Analysis of the received signal for an AR(p) clutter model

In order to address the selection of the two phase codes, we first focus our attention on the analytical expression of the received signal r when the clutter is modeled by an AR(p)[2] defined as follows:

$$x_n = \sum_{i=1}^{p} a_i x_{n-i} + u_n \tag{6}$$

with u_n a zero-mean complex white Gaussian noise with variance σ_u^2. Using this kind of model is of interest for the following reasons:
1/ It is well suited for Gaussian clutters [10],
2/ Different types of clutters can be simulated by modifying the AR parameters. However, the parameters must be selected such that stability is satisfied. Among the well-known criteria, one can first select the poles inside the unit circle in the z-plane and then deduce the AR parameters, e.g. $|a_1| < 1$ for an AR(1). As an alternative, one can directly analyze the set of AR parameters. Thus, for an AR(2) process, a_1 and a_2 have to be in the so-called stability triangle [11].
3/ The analytical expression of the inverse covariance matrix $\mathbf{\Gamma}^{-1}$ can be used to analyze the properties of the received signal. Thus, $\mathbf{\Gamma}^{-1}$ is given by [12]:

$$\mathbf{\Gamma}^{-1} = \frac{1}{\sigma_u^2} (\mathbf{F}\mathbf{F}^H - \mathbf{G}\mathbf{G}^H) \tag{7}$$

with:

$$\mathbf{F} = \mathbf{I} - \sum_{i=1}^{p} a_i \mathbf{J}^i \quad \text{and} \quad \mathbf{G} = -\sum_{i=1}^{p} a_i \mathbf{J}^{KNM-i} \tag{8}$$

Given (4), (7) and (8), and assuming that the thermal noise is negligible compared to the clutter, i.e. $\mathbf{M}^{-1} \approx \mathbf{\Gamma}^{-1}$, let us show that the received signal $r(\ell_0, \ell)$ can be approximated up to the factor $1/\sigma_u^2$ by the difference of two terms:
1/ A first one denoted r_1 which is due to $\mathbf{F}\mathbf{F}^H$ in (7). It only depends on the difference $\ell - \ell_0$. This property is of real interest at the receiver as we do not know the target position and so the value of ℓ_0. If the target is located in another range cell $\ell_0 + \Delta_{\ell_0}$, then r is shifted by Δ_{ℓ_0};
2/ A second term denoted r_2 which is due to $\mathbf{G}\mathbf{G}^H$ in (7). It does not satisfy the above property. However, we are going to show that it is equal to zero in many cases.

Proof of the first property: $r_1(\ell_0, \ell) = r_1(\ell_0 - \ell) = r_1(\lambda)$

Substituting (7) in (4), r_1 is defined as:

$$r_1(\ell_0, \ell) = (\mathbf{c} \otimes \mathbf{e}_1 \otimes \mathbf{d})^H (\mathbf{J}^{\ell_0})^H \mathbf{F}\mathbf{F}^H \mathbf{J}^{\ell} (\mathbf{c} \otimes \mathbf{e}_1 \otimes \mathbf{d}) \tag{9}$$

By replacing (8) in (9) and by introducing the variable $\lambda = \ell_0 - \ell$, after some developments and simplifications, one can show that:

$$r_1(\ell_0, \ell) = r_1(\lambda) = \sum_{q=-p}^{p} \alpha_q r_{\mathbf{c} \otimes \mathbf{e}_1 \otimes \mathbf{d}}(\lambda + q) \tag{10}$$

[2] It should be noted that x_n can be seen as the output of the infinite impulse response (IIR) filter whose input is u_n and whose transfert function is: $H(z) = \frac{1}{1 - \sum_{i=1}^{p} a_i z^{-i}} = \frac{1}{\prod_{i=1}^{p}(1 - p_i z^{-i})}$ with p_i the poles of $H(z)$.

where the coefficients α_q are given by:

$$\alpha_q = \begin{cases} 1 + \sum_{n=1}^{p} a_n^2 & q = 0 \\ -a_{|q|} + \sum_{n=1}^{p-|q|} a_n a_{n+|q|} & 0 < |q| \leqslant p-1 \\ -a_p & |q| = p \end{cases} \quad (11)$$

and $r_{\mathbf{c}\otimes\mathbf{e}_1\otimes\mathbf{d}}$ denotes the autocorrelation function of the sequence $\mathbf{c}\otimes\mathbf{e}_1\otimes\mathbf{d}$ which satisfies:

$$r_{\mathbf{c}\otimes\mathbf{e}_1\otimes\mathbf{d}}(\lambda) = \sum_{k=-K+1}^{K-1} r_{\mathbf{c}}(k) r_{\mathbf{d}}(\lambda - kMN) \quad (12)$$

with $r_{\mathbf{c}}$ and $r_{\mathbf{d}}$ the autocorrelation functions of the phase codes $\mathbf{c}$ and $\mathbf{d}$ respectively.
It should be noted that r_1 can be seen as the autocorrelation function of the sequence $\mathbf{c}\otimes\mathbf{e}_1\otimes\mathbf{d}$ after it has been filtered by the finite impulse response (FIR) filter of impulse response $[1 \;\; -a_1 \;\ldots\; -a_p]$.

In addition, including (12) in (10), r_1 can be rewritten as follows:

$$r_1(\lambda) = \sum_{k=-K+1}^{K-1} r_{\mathbf{c}}(k) \left(\sum_{q=-p}^{p} \alpha_q r_{\mathbf{d}}(\lambda + q - kMN) \right) \quad (13)$$

Introducing the function $f(\lambda) = \sum_{q=-p}^{p} \alpha_q r_{\mathbf{d}}(\lambda + q)$, (13) becomes:

$$r_1(\lambda) = \sum_{k=-K+1}^{K-1} r_{\mathbf{c}}(k) f(\lambda - kMN) \quad (14)$$

At that stage, let us look at the properties of $r_1(\lambda)$: as $\mathbf{d}$ is of size M, $r_{\mathbf{d}}(\lambda) = 0$ when $|\lambda| \geqslant M$. Thus, $f(\lambda) = 0$ when $|\lambda| \geqslant M + p$. Provided that $N \geqslant 3$ and $M \geqslant 2p$, there is no overlap between the pattern $f(\lambda)$ and its shifted versions, see Fig. (3).

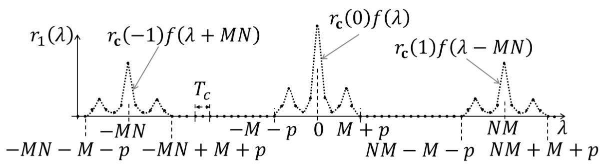

Fig. 3. Representation of $r_1(\lambda)$

As shown on Fig. (3), the k^{th} received pulse after processing is proportional to $r_{\mathbf{c}}(k)$. This property will be useful for the selection of the interpulse phase code, see section 3.1.

Proof of the second property: $r_2(\ell_0, \ell) = 0$ for some ℓ_0

From (4) and (7), $r_2(\ell_0, \ell)$ is given by:

$$r_2(\ell_0, \ell) = (\mathbf{c}\otimes\mathbf{e}_1\otimes\mathbf{d})^H (\mathbf{J}^{\ell_0})^H \mathbf{G}\mathbf{G}^H \mathbf{J}^{\ell} (\mathbf{c}\otimes\mathbf{e}_1\otimes\mathbf{d}) \quad (15)$$

For any order p, we can show that r_2 does not depend on the difference $\ell_0 - \ell$. For instance for an AR(2), (15) becomes:

$$\begin{aligned} r_2(\ell, \ell_0) = \frac{-1}{\sigma_u^2} (\mathbf{c}\otimes\mathbf{e}_1\otimes\mathbf{d})^H (\mathbf{J}^{\ell_0})^H \Big[& a_1 a_2 \tilde{\mathbf{e}}_1 \tilde{\mathbf{e}}_2^H + a_1 a_2 \tilde{\mathbf{e}}_2 \tilde{\mathbf{e}}_1^H \\ & + (a_1^2 + a_2^2) \tilde{\mathbf{e}}_1 \tilde{\mathbf{e}}_1^H + a_2^2 \tilde{\mathbf{e}}_2 \tilde{\mathbf{e}}_2^H + a_1 a_2 \tilde{\mathbf{e}}_{KNM} \tilde{\mathbf{e}}_{KNM-1}^H \\ & + (a_1^2 + a_2^2) \tilde{\mathbf{e}}_{KNM} \tilde{\mathbf{e}}_{KNM}^H + a_2 a_1 \tilde{\mathbf{e}}_{KNM-1} \tilde{\mathbf{e}}_{KNM}^H \\ & + a_2^2 \tilde{\mathbf{e}}_{KNM-1} \tilde{\mathbf{e}}_{KNM-1}^H \Big] \mathbf{J}^{\ell} (\mathbf{c}\otimes\mathbf{e}_1\otimes\mathbf{d}) \end{aligned} \quad (16)$$

with $\tilde{\mathbf{e}}_m, m = 1..., KNM$ the $KNM \times 1$ canonical basis vectors. Nevertheless, given the sparsity of the sequence $\mathbf{c}\otimes\mathbf{e}_1\otimes\mathbf{d}$ and the structure of $\mathbf{G}\mathbf{G}^H$, it can be shown that:

$$r_2(\ell, \ell_0) = 0 \quad \forall \ell_0 \in \Omega \quad (17)$$

with $\Omega = \big\{[p; MN - 1 - M - p] \cup [kMN; kMN - 1 - M - p], k \in [1; K-1]\big\}$.
In other words, $r_2(\ell, \ell_0) = 0$ when the target neither lies in the first p range gates of the first recurrence, nor in the last $M+p$ range gates of each recurrence. In that case:

$$r(\ell_0, \ell) \approx \frac{1}{\sigma_u^2} r_1(\ell_0 - \ell) \quad (18)$$

(18) is a key property used in the next section for the selection of $\mathbf{c}$ and the optimization of $\mathbf{d}$.

3. SELECTION OF THE INTER AND INTRAPULSE PHASE CODES

3.1. Choosing the interpulse phase code c to increase the unambiguous range

In this subsection, we first illustrate with an example how to increase the unambiguous range when the phase-coded received signal is altered by thermal noise only. Then, we show how this method could be applied for a colored Gaussian clutter modeled by an AR(p).

First case: thermal noise only

Depending on the correlation properties of $\mathbf{c}$, various cases can occur. Two examples of the received signal after matched filtering (MF) are represented on Fig. (4), where $d_m = 1, \forall m \in [0; M-1]$.

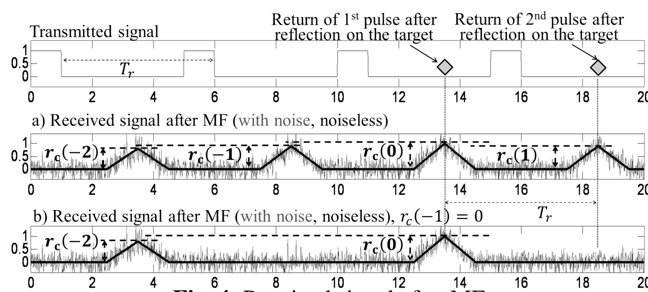

Fig. 4. Received signal after MF

On Fig. (4), case a), the main peak and the neighboring peaks cannot be distinguished, hence the range ambiguity is equal to $cT_r/2$. However, by choosing $\mathbf{c}$ such that:

$$r_{\mathbf{c}}(-1) = 0 \quad (19)$$

the unambiguous range is multiplied by two, see Fig. (4), case b). The constraint (19) is satisfied for odd values of K. Indeed, when K is even, the computation of $r_{\mathbf{c}}(-1)$ corresponds to the sum of $K-1$ terms that are equal to $+1$ or -1. Such a sum cannot be equal to 0. For any odd values of K, one solution is for instance the code whose $(K+1)/2$ first elements are "-1" and the $(K-1)/2$ others alternate from "+1" to "-1".

Second case: colored Gaussian clutter and thermal noise

From (14), (17) and (18), and following the same reasoning as in the thermal noise case, the ambiguous range can be doubled, i.e. it is equal to $2 \times cT_r/2$, provided K is odd.

In order to generalize this approach so that the unambiguous range becomes equal to $k \times cT_r/2$, with k an integer such that $k \leqslant K$, we could choose the codes that satisfy :

$$r_{\mathbf{c}}(-1) = r_{\mathbf{c}}(-2) = ... = r_{\mathbf{c}}(-k+1) = 0 \quad (20)$$

However, such codes do not exist. Indeed, assuming a phase code $\mathbf{c}$ of odd length K, the computation of $r_{\mathbf{c}}(2)$ corresponds to the sum of $K-2$ terms that are equal to $+1$ or -1. Such a sum cannot be equal to 0.

Among the possible alternatives, we could look at the relevance of the relaxed constraint:

$$r_{\mathbf{c}}(-1) \leqslant 1,\ r_{\mathbf{c}}(-2) \leqslant 1,\ ...,\ r_{\mathbf{c}}(-k+1) \leqslant 1 \qquad (21)$$

This kind of problem has been studied in the litterature and led to the Barker codes, which meet this constraint with $k = K$ but exist only for $K \in \{2, 3, 4, 5, 7, 11, 13\}$.

Given this brief study, we can conclude that the unambiguous range can be at least multiplied by 13. For greater values of K, we are currently investigating how to improve this result in order to guarantee a value for k given K.

3.2. Automatic selection of the intrapulse phase code combining a multiobjective approach and fuzzy logic

General approach

For the choice of $\mathbf{d}$ among the 2^M different phase codes, we suggest optimizing the following criteria related to r: 1/ the maximization of the mainlobe height, which is equivalent to maximizing the probability of detection, 2/ the minimization of the mainlobe width, which improves the range resolution, 3/ the minimization of the highest sidelobe, which contributes to the reduction of false alarm detections.

These three criteria are related to the first received pulse, i.e. λ such that $r_1(\lambda) = r_{\mathbf{c}}(0)f(\lambda)$ in (14). Note that the code $\mathbf{c}$ does not take part in the optimization. Furthermore, the optimization is only possible when $r_2(\ell_0, \ell) = 0$. We consider a multiobjective approach in order to select the intrapulse phase codes $\mathbf{d}$.

Let S_M be the set of all binary phase codes of length M. The Pareto front $\mathcal{P}$ is computed by going exhaustively through S_M and keep the non-dominated solutions defined as the solutions such that there is no other phase code that can simulaneously improve one or more criteria without degrading the others. $\mathcal{P}_2$ and $\mathcal{P}_3$ which are the Pareto fronts of 2nd and 3rd orders are then computed on the sets $S_M \backslash \mathcal{P}$ and $S_M \backslash (\mathcal{P} \cap \mathcal{P}_2)$ respectively.

In order to study the robustness of the three Pareto fronts to clutter variations, we compute $\mathcal{P}$, $\mathcal{P}_2$ and $\mathcal{P}_3$ for several values of the AR parameters which are gathered in the set $\mathcal{D}$. Then, we compute the percentages of presence of each code $\mathbf{d}$ in the sets of $\mathcal{P}$, of $\mathcal{P}_2$ and of $\mathcal{P}_3$. Our purpose is to automatically find the most robust phase codes to clutter variations. In other words, we seek the phase code $\mathbf{d}$ which is the most often in the set of $\mathcal{P}$, then the most often in the set of $\mathcal{P}_2$ and then the most often in the set of $\mathcal{P}_3$. We also want the phase code to remain the most often on one of the Pareto fronts when the AR parameters vary. Denoting p_1, p_2 and p_3 the percentages of presence in $\mathcal{P}$, $\mathcal{P}_2$ and $\mathcal{P}_3$, this relation of order is tantamount to seeking the code $\mathbf{d}$ which maximises p_1, then p_2 and then p_3, and maximizes also $p_1 + p_2 + p_3$. To obtain a score for each code that would make it possible to sort them, we use the fuzzy logic operators [13]. A pessimistic operator such as the min function or an optimistic operator such as the max function are not suitable because they do not take into account the sum $p_1 + p_2 + p_3$. It is also the case for reinforcement operators such as the "triple pi" operator. Rather, we choose a neutral operator such as the weigthed mean so as to emphasize the importance of the codes that belong to $\mathcal{P}$ compared to $\mathcal{P}_2$ or $\mathcal{P}_3$. In the next section, we present simulation results.

Discussion on the set $\mathcal{D}$ of AR parameters to be considered

A first scenario would be to assume that the clutter can have any kind of spectrum for a given order p. In that case, $\mathcal{D}$ corresponds to the stability domain. However, this scenario may be too general.

As an alternative, one can take advantage of some *a priori* information concerning the clutter. Indeed, using previous clutter data, we can deduce the estimations of the model order $\hat{p}$, the AR parameters $\{\hat{a}_i\}_{i=1,...,\hat{p}}$ or equivalently the poles $\{\hat{p}_i\}_{i=1,...,\hat{p}}$, as well as the variance of the driving process (by means of the Akaike or the MDL criteria, the Yule-Walker equations, etc.). Either $\mathcal{D}$ is reduced to $\{\hat{a}_i\}_{i=1,...,\hat{p}}$, or, to make the approach more robust, we can extend $\mathcal{D}$ to the set of clutter models defined by the set of AR parameters corresponding to the set of poles $\hat{p}_i + \Delta_{\hat{p}_i}$ with $\Delta_{\hat{p}_i}$ small and taken such that $|\hat{p}_i + \Delta_{\hat{p}_i}| < 1$ to guarantee the stability.

4. SIMULATIONS: CHOICE OF THE INTRAPULSE PHASE CODE

For the automatic selection algorithm, we test two sets of weights for the fuzzy logic operator:

(a) The weighted sum $0.5p_1 + 0.3p_2 + 0.2p_3$,

(b) The weighted sum $0.6p_1 + 0.3p_2 + 0.1p_3$.

In the following, $\mathbf{d}^{(i)}, i = 0, ..., 2^M - 1$ denotes the applicant codes that could be considered for the intrapulse phase code. $\mathbf{d}^{(i)}$ is the numerical value of i expressed in the base-2 numeral system on M bits and where the zeros are replaced by -1, i.e. $\mathbf{d}^{(0)} = [-1\ -1\ ...\ -1\ -1]^T$, $\mathbf{d}^{(1)} = [-1\ -1\ ...\ -1\ 1]^T$,..., $\mathbf{d}^{(2^M-1)} = [1\ 1\ ...\ 1\ 1]^T$. Due to the symmetry of the function $r(\ell_0, \ell)$, $\mathbf{d}^{(i)}$ and its opposite $\mathbf{d}^{(2^M-1-i)}$ yield the same result hence the simulations are run on 2^{M-1} codes. For the two scenario, $M = 13$, $K = 7$ and $N = 10$.

First scenario

In this first simulation protocol, $p = 2$ and $\mathcal{D}$ is the stability triangle. $\sigma^2 = 10^{-4}$ and $p = 2$. The variance σ_u^2 of the driving process is chosen so that the autocorrelation function of the AR processes taken at the lag 0 is equal to 1.

Both methods (a) and (b) give the same results and the first 3 phase codes are $\mathbf{d}^{(128)}$, $\mathbf{d}^{(16)}$ and $\mathbf{d}^{(512)}$.

Second scenario

Let us consider a set of real clutter data. The estimated model order is equal to 5. The AR parameters are then deduced from the estimated correlation function by means of the Yule-Walker equations. $\mathcal{D}$ is then obtained by generating 40 other set of AR parameters whose poles are "close" to the $\{\hat{p}_i\}_{i=1,...,5}$. The first 3 phase codes are $\mathbf{d}^{(1365)}$, $\mathbf{d}^{(1208)}$ and $\mathbf{d}^{(3755)}$.

5. CONCLUSIONS AND PERSPECTIVES

In this paper, our purpose is to simultaneously address the optimization of the waveform in terms of probability of detection/false alarm detections, range resolution and range ambiguity. The approach we propose includes a specific waveform combining an interpulse code of size K with an intrapulse code of size M and an AR modeling of the Gaussian clutter. This specific structure may reduce the space of applicant solutions but has the advantage of addressing the problems seperately. In addition, from the point of view of the implementation, this combination is "simpler". The waveform optimization we propose can be done offline so as to avoid having a too-heavy optimization algorithm running on the embedded system.

Among the possible perspectives, we could investigate the case of a non-Gaussian clutter that could be modeled by a spherically invariant random vector (SIRV) the speckle of which could be an AR process.

6. REFERENCES

[1] F. Le Chevalier, *Principles of radar and sonar signal processing*, Artech House, 2002.

[2] S. De Nicola, Y. Huang, A. De Maio, S. Zhang, and A. Farina, "Code optimization with similarity and accuracy constraints," in *Proc. of the IEEE Radar Conf.*, 2008, pp. 1–6.

[3] A. De Maio, S. De Nicola, Y. Huang, L. Zhi-Quan, and S. Zhang, "Design of phase codes for radar performance optimization with a similarity constraint," *IEEE Trans. on Sig. Process.*, vol. 57, no. 2, pp. 610–621, 2009.

[4] N. Levanon and E. Mozeson, *Radar signals*, Wiley, 2004.

[5] L. K. Patton, S. W. Frost, and B. D. Rigling, "Efficient design of radar waveforms for optimised detection in coloured noise," *IET Radar, Sonar and Navig.*, vol. 6, no. 1, pp. 21–29, 2012.

[6] J. Stringer, G. Lamont, and G. Akers, "Multi-objective evolutionary algorithm determined radar phase codes," in *Radar Conf. (RADAR), 2012 IEEE*, 2012, pp. 161–166.

[7] T. Rouffet, P. Vallet, E. Grivel, C. Enderli, B. Joseph, and S. Kemkemian, "Design of a multi-resolution phase-coded waveform in the presence of a colored gaussian clutter," in *Proc. of the IEEE Radar Conf.*, 2014.

[8] S. A. Hovanessian, "An algorithm for calculation of range in multiple PRF radar," *IEEE Trans. on Aerosp. and Elec. Syst.*, vol. AES-12, no. 2, pp. 287–290, 1976.

[9] N. Levanon, "Mitigating range ambiguity in high PRF radar using inter-pulse binary coding," *IEEE Trans. on Aerosp. and Elec. Syst.*, vol. 45, no. 2, pp. 687–697, 2009.

[10] J. B. Billingsley, *Low-angle radar land clutter, measurements and empirical models*, William Andrew Publishing, 2002.

[11] M. Najim, *Digital filters design for signal and image processing*, Wiley, 2006.

[12] I. C. Gohberg and A. A. Semencul, "On inversion of finite-section toeplitz matrices and their continuous analogues," *Matem Issled*, vol. 7, no. 2, pp. 201–223, 1972.

[13] J. Li, K. L. Butler-Purry, C. L. Benner, and B.D. Russell, "Selecting a fuzzy aggregation operator for multicriteria fault location problem," in *Proc. of the IEEE PES Power Systems Conf. and Exposition*, 2004, vol. 3, pp. 1476–1482.